

# Magnetohydrodynamic Mixed Convective Flow in a Cavity

R.YadollahiFarsani, B. Ghasemi

**Abstract**—A magnetohydrodynamic mixed convective flow in a cavity was studied in this paper. The lower surface of cavity was heated from below whereas other walls of the cavity were thermally isolated. The governing two-dimensional flow equations have been solved by using finite volume code. The effects of magnetic field were studied on flow and temperature field and heat transfer performance at a wide range of parameters, Such as Hartmann ( $0 \leq Ha \leq 100$ ) and Reynolds ( $1 \leq Re \leq 100$ ) numbers. The results showed that as Hartman number increases the Nusselt number, representing heat transfer from the cavity decreases.

**Keywords**—Cavity, Magnetic Field, Mixed Convection, Magnetohydrodynamic

## I. INTRODUCTION

THE study of mixed convection of electrically-conducting fluids in the magnetohydrodynamic (MHD) devices such as coolers of nuclear reactors, thermal insulators and micro-electronic devices should account for the effect of a transverse magnetic field on the fluid flow and the heat transfer mechanism. It has been found that the fluid flow experiences a Lorentz force due to the influence of the magnetic field. There has been an increasing interest to understand the magneto hydrodynamic convective heat transfer of electrically-conducting fluids in cavities [1]-[5]. The common finding of all these studies is that the magnetic field can suppress the convective flow field within the cavity and that the magnetic field is one of the important factors in the examination of the thermal performance of the cavity. M.Pirmohammadi et al. [6] numerically investigated the characteristic of free convection heat transfer in a cavity that was under the influence of transverse magnetohydrodynamic effects. Their study showed as the value of Hartman number increases, the free convection heat transfer into the cavity reduces. Despite the previous efforts, some aspects of fundamental knowledge of magnetohydrodynamic mixed convection heat transfer in cavities were still unknown; therefore this work was concerned with the effects of magnetic field on the laminar mixed convection flow in a cavity. The results were presented for a wide range of values of magnetic field strength. Results were presented graphically in terms of streamlines and isothermal lines. Finally the average Nusselt number at the heated surface of the cavity was calculated.

F.R.Yadollahi Farsani is with the, Ardal Centre, Shahrekord Branch, Islamic Azad University–Shahrekord –Iran. (Phone: +983813332901; fax: +983826224041; e-mail: r.yadollahi@iaushk.ac.ir).

S. B. Ghasemi is with Department of Engineering, Shahrekord University, Shahrekord, P.O.Box 115, Iran. (e-mail: Behzadgh@yahoo.com).

TABLE I  
SYMBOLS AND UNITS

Symbol	Quantity
$g$	gravitational acceleration, [ $m/s^2$ ]
$P$	pressure [Pa]
$T$	temperature [ $^{\circ}C$ ]
$L$	cavity Width [m]
$Nu$	local Nusselt number
$Nu_m$	average Nusselt number
$B_0$	magnetic field strength
$Pr$	Prandtl number, $\nu/\alpha$
$Gr$	Grashof number, $g\beta\Delta\theta L^3/\nu^2$
$Re$	Reynolds number, $u_0 L/\nu$
$Ha$	Hartman number, $(B_0 L \sqrt{\sigma/\rho\nu})$
$x, y$	Cartesian coordinates (m)
$X, Y$	non dimensional coordinates
$u, v$	velocity components ( $ms^{-1}$ )
$U, V$	dimensionless velocities in X and Y direction( $m/s$ )
$\alpha$	effective thermal diffusivity fluid [ $m^2s^{-1}$ ]
$\beta$	coefficient of thermal expansion of fluid [ $K^{-1}$ ]
$\Delta\theta$	temperature difference [ $K^{-1}$ ]
$\theta$	dimensionless temperature, $T-T_c/T_h-T_c$
$\mu$	effective dynamic viscosity [ $Pa s^{-1}$ ]
$\tau$	Dimensionless time
$\rho$	fluid density [ $kgm^{-3}$ ]

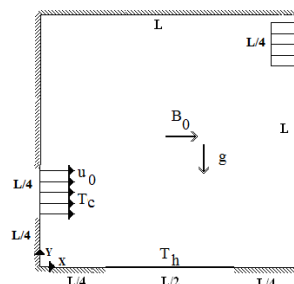


Fig. 1 Schematic diagram of the problem

## II. MODEL SPECIFICATION

The geometry considered in this study was a two-dimensional horizontal cavity with (Fig. 1). The length of the cavity ( $L$ ) was considered as the reference length in the dimensional analysis. The width of the cavity was equal to its length. The inlet and the outlet of the cavity were located at a distance of  $L/4$  and  $3L/4$  respectively from the bottom of the cavity. The height of the inflow and outflow openings is ( $L/4$ ). Air was introduced to the cavity at a uniform velocity ( $u_0$ ) and temperature ( $T_c$ ). The flow was assumed to be laminar and incompressible with the Prandtl number of  $Pr=0.71$ . The radiation effects were assumed to be negligible. a length of  $L/2$  of the cavity's bottom wall was heated at a constant temperature ( $T_h$ ). The rest walls of the cavity were thermally insulated. A uniform magnetic field with the strength of  $B_0$  was

applied in the same direction of the inflow. All the thermo-physical properties of the air flow were assumed constant except for the variation in density with temperature, where a Boussinesq approximation was applied. Fully-developed conditions were considered at the exit section of the cavity and no-slip boundary conditions ( $U=V=0$ ) were assumed on all the walls.

III. EQUATIONS

The nature of the magnetohydrodynamic flows includes both fluid dynamics (Navier–Stokes) and electrodynamics (Maxwell) equations. Lorentz force and Ohm’s law have been considered in these equations. The Ohm’s law was taken into consideration and the magnetic Reynolds number of the flow was taken to be small so that the flow induced distortion of the applied magnetic field can be neglected. The additional field induced by the fluid motion was weak compared with respect to the applied field. The non-dimensional forms of continuity, momentum and energy equations describing the flow under Boussinesq approximation are as follows:

$$\frac{\partial U}{\partial X} + \frac{\partial V}{\partial Y} = 0 \tag{1}$$

$$U \frac{\partial U}{\partial X} + V \frac{\partial U}{\partial Y} = -\frac{\partial P}{\partial X} + \frac{1}{Re} \left( \frac{\partial^2 U}{\partial X^2} + \frac{\partial^2 U}{\partial Y^2} \right) \tag{2}$$

$$U \frac{\partial V}{\partial X} + V \frac{\partial V}{\partial Y} = -\frac{\partial P}{\partial Y} + \frac{1}{Re} \left( \frac{\partial^2 V}{\partial X^2} + \frac{\partial^2 V}{\partial Y^2} \right) + \frac{Gr}{Re^2} \theta - \frac{Ha^2}{Re} V \tag{3}$$

$$U \frac{\partial \theta}{\partial X} + V \frac{\partial \theta}{\partial Y} = \frac{1}{Re.Pr} \left( \frac{\partial^2 \theta}{\partial X^2} + \frac{\partial^2 \theta}{\partial Y^2} \right) \tag{4}$$

In the above equations, the following non-dimensional parameters are used:

$$X = \frac{x}{L}, \quad Y = \frac{y}{L}, \quad U = \frac{u}{u_o}, \quad V = \frac{v}{u_o}, \quad P = \frac{\bar{p}}{\rho u_o^2}, \quad Ha = B_o L \sqrt{\frac{\sigma}{\rho \nu}} \tag{5}$$

$$\theta = \frac{T - T_c}{T_h - T_c}, \quad Re = \frac{\rho u_o L}{\mu}, \quad Pr = \frac{\nu}{\alpha}, \quad \tau = \frac{u_o t}{L}, \quad Gr = \frac{g \beta (T_h - T_c) L^3}{\nu^2}$$

The term on the right-hand side of Eq. (3) includes the Lorentz force induced by the interaction of the magnetic field with the convective motion. The boundary conditions for the present problem were specified as follows:

- At the inlet:  $U = 1, V = 0, \theta = 0,$
- At the outlet: convective boundary condition:  
 $\partial U / \partial X = 0, \partial \theta / \partial X = 0, V = 0,$
- At top wall of channel:  $U = 0, V = 0, \theta = 0,$
- At the other walls:  $U = 0, V = 0, \partial T / \partial N = 0,$
- At the bottom of cavity:  $U = V = 0, \theta = 1,$

where N is the non-dimensional distances in both X and Y directions acting normal to the surface. The local Nusselt number at the heated surface was calculated by using  $Nu = -\partial \theta / \partial Y$ . The average Nusselt number was, therefore, obtained by integrating the Nusselt number over the cavity’s bottom wall as:

$$Nu_m = -(2/L) \int \partial \theta / \partial Y$$

IV. METHOD OF SOLUTION

The governing equations presented in Eqs. (1)-(4) along with the boundary conditions (Eq. (6)) were numerically solved by employing the finite volume method and using the staggered grid arrangement. The power law scheme, which was a combination of the central difference and the upwind schemes, was used to discrete the convection terms [7]. A staggered grid system, in which the velocity components are stored midway between the scalar storage locations, was used. The solution of the fully-coupled discretized equations was obtained iteratively using the TDMA method. In order to get the accurate solutions, the  $10^{-6}$  convergence condition was considered.

V. GRID INDEPENDENCE

The grid study test was performed at  $Gr=10^4, Ha =50$  for deferent Reynolds number. Table II shows the dependence of the Nusselt quantities on the grid size. The results show that a grid size of  $220 \times 220$  is adequate to ensure the grid independency.

TABLE II  
GRID INDEPENDENCE STUDY FOR  $Ha=50$  AND  $Gr = 10^4$

Grid	150×150	170×170	200×200	220×220	240×240
Re=1	0.98	1.24	1.5	1.62	1.65
Re=10	1.05	1.36	1.75	1.88	1.94
Re=100	1.98	2.14	3.14	3.26	3.34

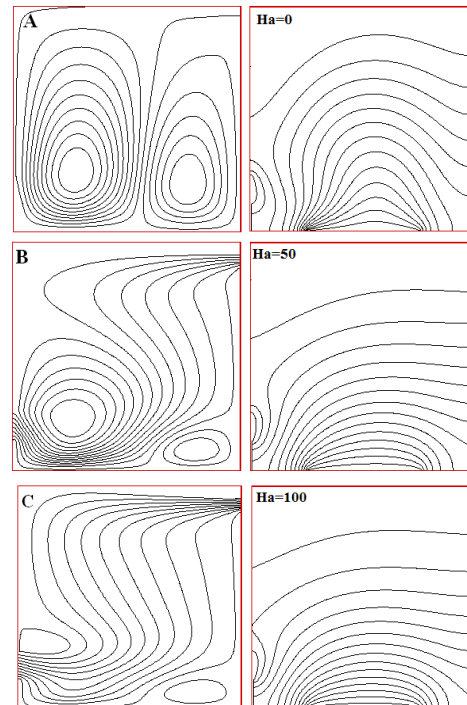


Fig. 2 Left, Streamlines and Right, Isotherms for (A)Ha=0,(B) Ha=50 and (C)Ha=100, whereas Re=1 and Gr= 10<sup>4</sup>

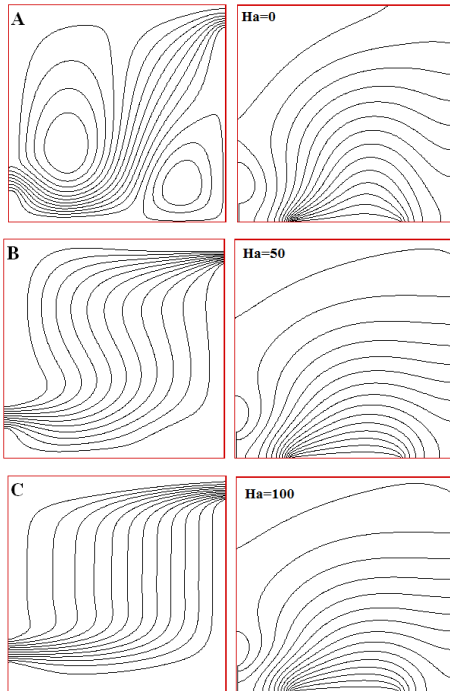


Fig. 3 Left, Streamlines and Right, Isotherms for (A)  $Ha=0$ , (B)  $Ha=50$  and, (C)  $Ha=100$ , at  $Re=10$  and  $Gr=10^4$

VI. RESULTS AND DISCUSSIONS

The results of the numerical analysis of the magneto hydrodynamic mixed convection in the channel with an open cavity for a range of values of the Reynolds number ( $1 \leq Re \leq 100$ ) and the Hartmann number ( $0 \leq Ha \leq 100$ ) at Grashof number ( $Gr=10^4$ ), are presented and the flow and temperature fields and the heat transfer performance of the channel are examined.

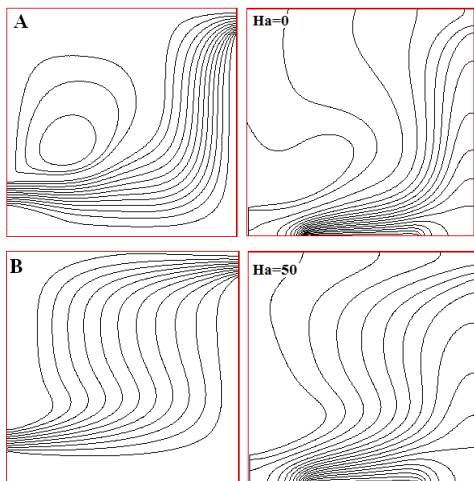


Fig. 4 Left, Streamlines and Right, Isotherms for (A)  $Ha=0$ , (B)  $Ha=50$  and, (C)  $Ha=100$ , at  $Re=100$  and  $Gr=10^4$

In this section the influence of the Hartmann number ( $Ha = 0, 50, 100$ ) on the flow and temperature fields for  $Gr=10^4$  and three values of the Reynolds number ( $Re=1, 10, 100$ ) are presented. Fig. 2 illustrates the streamlines and isotherms for  $Re = 1$ , where the buoyancy effects dominate the flow field in the cavity and the heat transfer is mainly due to natural convection. The results show that the buoyancy induced vortices in the cavity in the absence of the magnetic field ( $Ha = 0$ ). The vortices, however, start to decrease and the streamlines are extended between the inlet and the outlet of the cavity as the magnetic field is applied ( $Ha = 50$ ). The size of the vortices decreases and mainstream flow in cavity get strong as the Hartmann number increases to  $Ha = 100$ . The isotherms show thin thermal boundary layers in the vicinity of the cavity's bottom wall for  $Ha = 0$ . As the Hartmann number increases, the isotherms distribute more uniformly and smoothly between the bottom wall of the cavity and the top wall.

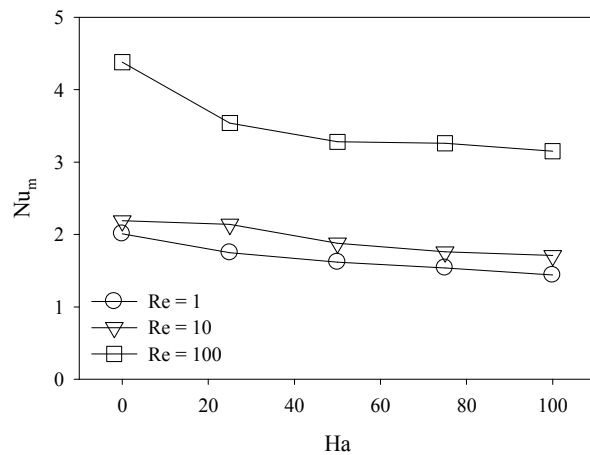


Fig. 5 Effect of Hartman number on average Nusselt number in the cavity for variant  $Re$ , at  $Gr=10^4$

Fig. 3 shows the streamlines and isotherms for  $Re = 10$ , where the contribution of the forced convection in the flow and temperature fields increases. Two vortices are evident inside of the cavity for  $Ha = 0$ . When the Hartmann number increases, both of them are vanished due to the effect of the magnetic field. The isotherms distribution is also affected by

the effect of the magnetic field. Less bend of the isotherms lines is observed as the Hartmann number increases.

Fig. 4 shows the streamlines and isotherms for  $Re = 100$ , where the forced convection dominates the flow and temperature fields. In the absence of the magnetic field, a large circulating cell is observed above mainstream flow in the cavity. As the Hartmann number increases, the vortex is vanished due to the effect of the magnetic field whereas the strength of mainstream flow increases. The density of the stratified isotherms near the bottom wall of the cavity decreases as the Hartmann number increases.

It has been observed that for all values of the Reynolds number, the intensity of isotherms in the vicinity of the cavity's bottom wall decreases as the Hartmann number increases. This suggests lower heat transfer rates for the cavity as the strength of the magnetic field increases. In order to examine the cavity's heat transfer performance, the values of the average Nusselt number ( $Nu_m$ ) at different Hartmann, Reynolds and Grashof numbers are presented in Fig. 5. The effect of magnetic field on the average Nusselt number ( $Nu_m$ ) for governing parameters  $Ha$ ,  $Gr$  and  $Re$  is shown in Fig 5. It is shown for various Reynolds number, the value of  $Nu_m$  decreases as Hartman number increases.

TABLE II  
AVERAGE NUSSLETT NUMBER DECREASE PERCENT AT  $Re=100$  AND  $Gr = 10^4$

	$Ha=0$	$Ha=25$	$Ha=50$	$Ha=75$	$Ha=100$
$Re=100$	4.38	3.54	3.28	3.26	3.15
Decrease of Average Nusselt number (%)		19	25	26	28

Also it's clear as the Reynolds number increases the Nusselt numbers, representing heat transfer from bottom of the cavity, increases.

In order to distinct the effect of magnetic field on average Nusselt number, the percent of decrease in average Nusselt numbers, at  $Re=100$  and  $Gr=10^4$  showed in table III. It's resulted that the effect of magnetic on mixed convection is so noticeable that magnetic field can't be undeniable in mixed convection heat transfer problems.

#### REFERENCES

- [1] O. Garandet, J. P., Alboussiere, T., and Moreau, R., 1992, "Buoyancy driven convection in a rectangular enclosure with a transverse magnetic field," *International Journal of Heat and Mass Transfer*, 35, 4, pp. 741-748.
- [2] Venkatachalappa, M., and Subbaraya, C. K., 1993, "Natural convection in a rectangular enclosure in the presence of a magnetic field with uniform heat flux from the side walls," *Acta Mechanica*, 96, 1-4, pp. 13-26.
- [3] Alchaar, S., Vasseur, P., and Bilgen, E., 1995, "Natural convection heat transfer in a rectangular enclosure with a transverse magnetic field," *Journal of Heat Transfer*, 117, 3, pp. 668-673.
- [4] Rudraiah, N., Barron, R. M., Venkatachalappa, M., and Subbaraya, C. K., 1995, "Effect of a magnetic field on free convection in a rectangular enclosure," *International Journal of Engineering Science*, 33, 8, pp. 1075- 1084.
- [5] Ghasemi, B., Aminossadati, S. M., and Raisi, A., 2011, "Magnetic field effect on natural convection in a nanofluid-filled square enclosure," *International Journal of Thermal Sciences*, 50, 9, pp. 1748-1756.
- [6] Pirmohammadi, M., Ghassemi, M., "Effect of magnetic field on convection heat transfer inside a tilted square enclosure". *International communication in Heat and Mass Transfer* 36,2009, pp. 776-780.
- [7] Patankar, S.V., "Numerical Heat Transfer and Fluid Flow", Hemisphere, Washington, DC, 1980.